Article ID:1004-4213(2010)09-1658-8

Remote Sensing Image Denoising Algorithm Based on Fusion Theory Using Cycle Spinning Contourlet Transform and Total Variation Minimization*

ZHAO Jie, YANG Jian-lei

(*College of Electronics and Information Engineering, Hebei University, Baoding, Hebei* 071002, *China*)

Abstract: In order to solve the problem that most of existing image denoising methods insufficiency preserve the details and enhance edges while implementing denoising, a new method for remote sensing image denoising is proposed, based on a combination of cycle spinning contourlet transform (CT), and the total variation (TV) minimization scheme. The proposed method relies on principles that CT scheme is well suited for preserving detailed and fine textures information of original image while TV minimization denoising scheme is capable of enhancing sharpened significant edges while denoising, therefore to fuse the two schemes using the proposed fusion rule can achieve better results. Compared with several commonly used approaches, the experimental results show that this novel algorithm is capable of reducing Gibbs phenomenon and staircase effect produced by CT and TV denoising methods respectively, superior both in visual quality of denoising and Peak Signal to Noise Ratio (PSNR), and preserves more spectral information and less spectral distortion simultaneously.

Key words: Remote sensing image; Contourlet transform; Cycle Spinning; Total variation minimization; Image denoising; Fusion

CLCN:TP391 **Document Code**:A **doi**:10.3788/gzxb20103909.1658

0 Introduction

Remote sensing image is an important data source about image analysis, urban mapping and fire monitoring, and also plays an increasingly fundamental role in many other fields. However, for remote sensing images being of huge data size, with abundant details, coding and long-distance wireless transmission from satellite to ground receiving stations, most of the remote sensing images have poor visual quality, and the detailed overwhelmed in the noise, therefore it is significant to implement denoising technique before the remote sensing images are analyzed.

As an important area of image processing, the image denoising technique was significantly improved for the introduction of wavelet transform. However, traditional two dimension wavelet is hard to represent sharp image transitions[1] and smoothness along the contours[2].

In recent years, some new methods have been introduced in order to represent higher dimensional image features, such as ridgelets, wedgelets, curvelets, contourlet[3]. Starck, Candès, and Donoho[4] employed the curvelet transform in the denoising task by using a translation invariant wavelet as the first stage of the curvelet transform. As the curvelet transform was proposed in continuous domain, it could not implement in the discrete domain easily. Do and Vetterli[2] utilized 2-D nonseparable filter banks and a directional multiresolution analysis framework to develop the contourlet transform (CT), which was employed for image denoising[5], fusion[6], enhancement[7-8] and multipurpose watermarking[9] effectively. It exhibits higher directional sensitivity and higher anisotropy and can more exactly capture the image edges to the different scale and frequency subbands than previous transforms.

R. R. Coifman and D. L. Donoho[10] employed the wavelet transform (WT) using cycle spinning (CSWT) in wavelet denoising, and experimental results demonstrate that method (CSWT) outperforms the original WT. In 2007, it was successfully applied for MRI image

*Supported by the Research and Development Projects of Science and Technology of Hebei Province(06242188D-2), the Natural Science Foundation of Hebei Province (F2007000221)

Tel:0312-5073113 Email:jiezhaohbu@126.com

Received date:2009-12-23 Revised date:2010-03-08

denoising[11].

Hence, R. Eslami, H. Radha[12] applied cycle spinning to compensate for the lack of translation invariance property of contourlet, and was successfully employed in image denoising and show significant improvements when compared to previous methods, especially for images comprising mostly detailed and fine textures. The contourlet transform using cycle spinning (CSCT) can reduce Gibbs phenomenon-like artifacts effectively but does not eliminate it. The CSCT is more suitable for image fusion, image denoising and other image processing.

Besides the denoising algorithms in transform domain, PDE or variational approach is another denoising category. One variational approach that has attracted a great deal of attention is the total variation method proposed by Rudin, Osher and Fatemi (ROF)[13], and they viewed that the total variation of the noise images is greater than the original images; consequently, the reconstruction of noise images can be considered as the problem of TV minimization, and the minimizer can preserve edges and allows for sharp boundaries, and at the same time it also do not introduce artifacts as a result of the Gibbs oscillation near discontinuities. However, it is not fully consistent with the morphological theory, and usually produces visible staircase effect in strong noise environment. Total variation has also been used to image enhancement[14] and feature extraction[15], etc.

In this paper, we propose a novel denoising algorithm for remote sensing images using fusion technology. In algorithm, we use CSCT denoising method to capture imperfect detailed and fine textures information of remote sensing images sufficiently and TV denoising approach can preserves edges and allows for sharp boundaries, and we employ the our fusion algorithm to fused the two denoised images. Experiments show that our algorithm can obtain better denoising performance, higher PSNR for noise remote sensing images.

2 The contourlet transform

The contourlet transform (CT) has been proposed by Vetterli and Do[2]. The contourlet is constructed by a double filter bank structure in which at first the Laplacian pyramid (LP) is used to capture the point discontinuities, and followed by a directional filter bank (DFB) to link point discontinuities into linear structure and the structure is also called Pyramidal Directional Filter Bank (PDFB)[4] as shown in Fig. 1(a).

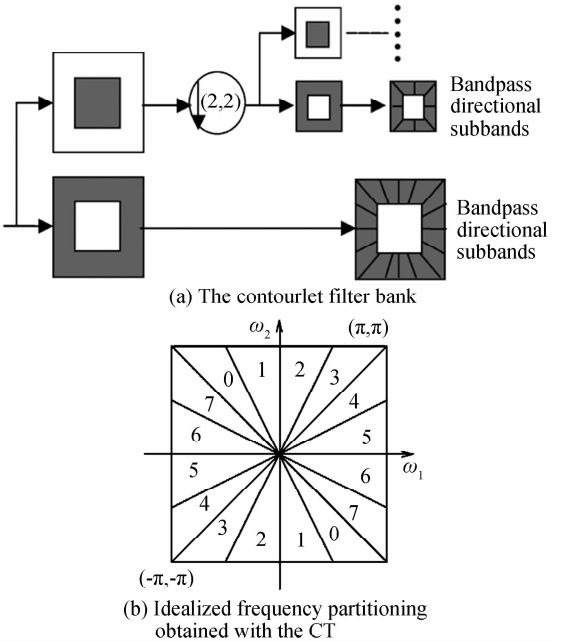

Fig. 1 Contourlet transform

In the frequency domain, the LP is used to complete a multi-scale decomposition. When a two dimensional image passes the LP, it is decomposed into an approximation image which contains low frequencies, or alternatively, is a coarse scale image and a detailed image which contains the complementary high frequencies, or alternatively, can be regarded as a fine scale image containing points discontinuities of the image, namely edge points.

The DFB is a set of filters that partition the 2D frequency domain into wedges at different orientations, or alternatively, decomposes each LP detail band into many directions (a power of 2) and combine singular point where located in the same direction into one coefficient. Fig. 1 (b) shows an example of the frequency decomposition achieved by the DFB, where $l=3$ and there are $2^3=8$ real wedge-shaped frequency bands.

3 The total variation minimization denoising algorithm

We assume u_o and u are two dimensional images defined on Ω which is an open subset of R^2 and they are modelled as

$$u_o = Au + \zeta \tag{1}$$

where u_o is an observed image, the variable u is the denoised image, A is a linear blur operator and ζ represents Gaussian white noise with zero mean and variance σ^2.

An equivalent problem to estimate the original

image u from an observed noisy image u_o is

$$\min_u \left\{ J(u) = \alpha J_{\mathrm{TV}}(u) + \frac{1}{2} \| Au - u_o \|_{L^2}^2 \right\} \tag{2}$$

Here, $J_{\mathrm{TV}} = \int_\Omega \sqrt{|\nabla u|^2 + \beta} \mathrm{d}x\mathrm{d}y$ and $\| \cdot \|$ is the norm on $L^2(\Omega)$, $\alpha > 0$ is the penalty parameter, $|\Omega|$ is the area of Ω, $\beta > 0$ is the diffusion regularization parameter that amend the small perturbations introduced by TV semi-norm and it is typically small.

Then the Euler-Lagrange equation for Eq. (2) is

$$-\alpha \nabla \cdot \left(\frac{\nabla u}{\sqrt{|\nabla u|^2 + \beta}} \right) + A^* (Au - u_o) = 0 \tag{3}$$

with $\partial u / \partial n = 0$, $x \in \partial\Omega$ and $x = [x \quad y]^T$, where A^* is the adjoint operator of A with respect to the L_2 inner product, $\partial\Omega$ is the boundary of Ω and ∂n is the normal vector of $\partial\Omega$.

4 The proposed denoising algorithm

From the analysis of CT principle, the CT has such advantages as flexible multiresolution, different directions at each scale, local and directional image expansion and can more effectively capture the geometric information of images than wavelet, ridgelet, curvelet and contourlet transform.

For the characteristics of remote sensing images, considering TV minimization is capable of preserving significant edges, which is fundamental for remote sensing image, and CSCT to capture imperfect detailed and fine textures information of remote sensing images sufficiently, consequently the combination of CSCT and TV denoising methods can achieve better results.

4.1 Cycle spinning contourlet denoising and fusion algorithms

From the above analysis we can see that contourlet transform is superior to wavelet, ridgelet, curvelet and contourlet transforms in many performances. However, due to downsamplers and upsamplers presenting in both the Laplacian pyramid and the DFB, the contourlet transform is not shift-invariant, therefore when contourlet is used for image denoising, the reconstructed image will appear visual fake, namely Gibbs phenomenon.

The Gibbs phenomenon is closely related with position of discontinuous point[10], so shift or change position of discontinuous points can decrease or eliminate Gibbs phenomenon and the denoised image is competent to be significantly improved. Nevertheless, the method can not eliminate the Gibbs phenomenon completely.

In the fusion process, it is also important to alleviate the problem and shows a considerable improvement of the fusion quality[16].

Suppose S is the noise image and let TV denote the TV denoising process, the proposed denoising algorithm in our paper can be written as the following equation

$$\hat{I} = \sum_{i=0,j=0}^{K_1,K_2} C_{-i,-j} \{ Ct^{-1} \{ Fu[Th(Ct(C_{i,j}(S)) \\ Ct(C_{i,j}(Tv(S)))] \} \} \tag{4}$$

where K_1 and K_2 are the maximal circular shift distance in the horizontal direction and the vertical direction respectively, Ct and Ct^{-1} denote the process of contourlet decomposition and reconstruction process respectively, $C_{i,j}(I)$ and $[C_{i,j}(I)]^{-1}$ are the cycle spinning operator and its reversible circular shift operator with i in the horizontal direction and j in the vertical direction respectively, then Th and Fu represent the coefficient threshold operator and fusion rule respectively.

In this paper, image decomposition is performed by the CSCT to compensate for the lack of translation invariance property of CT to improve the quality of the fusion image and denoised image.

4.2 The fusion rule of coefficients

Image fusion is the process of merging different or incomplete representations of the same object to form a single representation that shows a considerable improvement of the quality over the original representations.

After applying the TV denoising method to noisy remote sensing image S, we can obtain the denoised image S_{TV}, then implement CSCT to decompose the S_{TV} to obtain the coefficients $\{C^L_{\mathrm{TV}}(i,j), C^L_{\mathrm{TV}}(i,j;l,k)(1 \leqslant l \leqslant L)\}$.

Then decompose the image S using the CSCT with same scale and direction as S_{TV} decomposition, and perform the 3σ threshold on original coefficients to get the new coefficients $\{C^L_{\mathrm{CT}}(i,j), C^L_{\mathrm{CT}}(i,j;l,k)(1 \leqslant l \leqslant L)\}$.

In the two kinds of coefficients, $C^L_{\mathrm{TV}}(i,j)$ and $C^L_{\mathrm{CT}}(i,j)$ are the low frequency subband coefficients, and the $C^L_{\mathrm{TV}}(i,j;l,k)$ and $C^L_{\mathrm{CT}}(i,j;l,k)$ are the bandpass directional subband coefficients at the l-th scale and on the k-th direction of S_{TV} and S decomposition respectively, and (i,j) and L specify the location and the number of decomposition level, respectively.

The low frequency subband coefficients

determine the contour of the image and constructed the images' approximate information with little noise pollution, and it is significant to identify the different regions in remote sensing images, however, noisy and staircase/block effect in S and S_{TV} can result in many contours artificial and smooth, therefore a rule should be introduced to obtain distinct contours.

Region variance (RVA) maximum rule is a commonly used fusion rule in low frequency domain[17], and the RVA of$C^L_{\mathrm{TV}}(i,j)$ or $C^L_{\mathrm{CT}}(i,j)$ can be defined as follows

$$V^L_A(i,j)=\sum_{(x,y)\in\Omega(i,j)}(C^L_A(x,y)-\overline{C^L_A(i,j)}) \tag{5}$$

where $A=$ CSCT or TV, and $\Omega(i,j)$ is a small region with the coefficient $C^L_A(i,j)$ as the center, its size is 3×3 in our paper, and $\overline{C^L_A(i,j)}$ denotes the average of coefficients in $\Omega(i,j)$.

Suppose $C^L_F(i,j)$ is the fused low-frequency coefficients located at (i,j) in the l-th scale and k-th direction subband, and then the fusion rule can be described as follows

$$C^L_F(i,j)=w^L(i,j)\times C^L_{\mathrm{CSCT}}(i,j)+(1-w^L(i,j))\times C^L_{\mathrm{TV}}(i,j) \tag{6}$$

where $w^l_k(i,j)$ is the fusion weights of coefficients located at (i,j) in the l-th scale and k-th direction subband. $w^L_k(i,j)$ is expressed as follows

$$w^L_k(i,j)=\frac{V^L_{\mathrm{CSCT}}(i,j)}{(V^L_{\mathrm{CSCT}}(i,j)+V^L_{\mathrm{TV}}(i,j))} \tag{7}$$

In the frequency domain, both image details and noise produce high frequency subband coefficients, which contain main edges and texture feature information. Noise can lead to image gradient smaller and the gradient of the high frequency subband coefficients also smaller, image with greater values of gradient have higher visual quality, especially remote sensing images containing a lot of imperfect detailed and fine texture. In order to make full use of information in the neighborhood and the detailed and fine texture of two denoised images in the CSCT domain and superiority of preserving the edge of TV denoising algorithm, we use the following fusion rule.

Suppose the coefficient absolute value of $C^L_A(i,j;l,k)$ is $CAV^L_A(i,j;l,k)$ and $A=$ CSCT or TV, denoting different original coefficients.

When $CAV^L_{\mathrm{CSCT}}(i,j;l,k)>CAV^L_{\mathrm{TV}}(i,j;l,k)$, it may result from the noisy pollution in the CSCT high frequency domain or no, so we use the average region gradient (ARG) to identify that. If $CAV^{l,k}_{\mathrm{CSCT}}(i,j)\leqslant CAV^{l,k}_{\mathrm{TV}}(i,j)$, we conclude that it is produced by preserving edge of TV denoising algorithm. The rule is described as follows

If $CAV^{l,k}_{\mathrm{CSCT}}(i,j)>CAV^{l,k}_{\mathrm{TV}}(i,j)$ then

$$C^L_F(i,j;l,k)=\begin{cases}C^L_{\mathrm{CSCT}}(i,j;l,k) & \text{if } ARG^L_{\mathrm{CSCT}}(i,j;l,k)\geqslant ARG^L_{\mathrm{TV}}(i,j;l,k)\\ (C^L_{\mathrm{CSCT}}(i,j;l,k)+C^L_{\mathrm{TV}}(i,j;l,k))/2 & \\ \text{else} & \end{cases} \tag{8}$$

If $CAV^{l,k}_{\mathrm{CSCT}}(i,j)\leqslant CAV^{l,k}_{\mathrm{TV}}(i,j)$ then

$$C^L_F(i,j;l,k)=C^L_{\mathrm{TV}}(i,j;l,k) \tag{9}$$

In Eq. (8) and Eq. (9), $C^L_F(i,j;l,k)$ is the fused high-frequency coefficients located at (i,j) in the l-th scale and k-th direction subband. $ARG^L_A(i,j;l,k)(A=\mathrm{CSCT/TV})$ denotes the average region gradient in the square window with the coefficient $C^L_A(i,j;l,k)(A=\mathrm{CSCT/TV})$ as the center, its size is 3×3 in our paper, defined as

$$ARG^L_A(i,j;l,k)=\frac{1}{(M-1)(N-1)}\sum_{i=1}^{M-1}\sum_{j=1}^{N-1}\sqrt{\frac{\Delta I_x^2+\Delta I_y^2}{2}} \tag{10}$$

where $M\times N$ is the size of the square window with coefficient $C^L_A(i,j;l,k)(A=\mathrm{CSCT/TV})$ as the center, and ΔI_x and ΔI_y are the first-order differential on x and y direction respectively, described as follows

$$\Delta I_x=C^L_A(i,j;l,k)-C^L_A(i-1,j;l,k) \tag{11}$$

$$\Delta I_y=C^L_A(i,j;l,k)-C^L_A(i,j-1;l,k) \tag{12}$$

The detailed procedure to perform the proposed algorithm is described as follows:

Step 1 Carry out the TV denoising algorithm to image S, obtain the denoised image S_{TV}, and compute the CSCT decomposition to the image S_{TV} for L levels to obtain the coefficients $\{C^L_{\mathrm{TV}}(i,j), C^L_{\mathrm{TV}}(i,j;l,k)(1\leqslant l\leqslant L)\}$.

Step 2 Perform CSCT denoising algorithm for image S to get the denoised coefficients $\{C^L_{\mathrm{CT}}(i,j), C^L_{\mathrm{CT}}(i,j;l,k)(1\leqslant l\leqslant L)\}$.

Step 3 Apply Eq. (6), Eq. (8) and Eq. (9) to fuse the coefficients $C^L_{\mathrm{TV}}(i,j)$ and $C^L_{\mathrm{CT}}(i,j)$,$C^L_{\mathrm{TV}}(i,j;l,k)$ and $C^L_{\mathrm{CT}}(i,j;l,k)$, and obtain the final denoised coefficients $\{C^L_F(i,j),C^L_F(i,j;l,k)(1\leqslant l\leqslant L)\}$.

Step 4 Perform inverse CSCT to reconstruct the denoised image from the coefficients $\{C^L_F(i,j), C^L_F(i,j;l,k)(1\leqslant l\leqslant L)\}$.

In the visible portion of the light spectrum, the predominant colors are red, green and blue, and the RGB color space is the most commonly used spaces of all the color spaces (i. e., LHS, HSI, YIQ, etc.) to represent color images, so we consider the color remote sensing images as RGB color images in this paper.

Above mentioned steps are designed for panchromatic remote sensing images, if remote sensing images are multi-spectral images, apply the step1 to step 4 mentioned above to R, G, B components respectively and get the new R′, G′ and B′, then use the R′, G′ and B′ to reconstruct the denoised images.

5 Experimental results and discussion

In order to show the denoising performance of the proposed algorithm, we selected panchromatic and multi-spectral remote sensing image for our experience. For the denoising performance of the CSCT outperforms the WT and CSWT to a large extent[12], we have not compared our algorithm with WT and CSWT, but with CT, CSCT and TV denoising approaches, by using the threshold $T=3\sigma$ for CT and CSCT. In the experiments, '9-7' and 'pkva' filters are used in pyramidal and directional decomposition, respectively, and for contourlet transform, we used 6 LP levels and 64 directions in the finest level.

Visual and quantitative comparisons are two major means to evaluate the quality of images. In this section, we compare the proposed method with the other ones in terms of both visual and quantitative measurements.

For the remote sensing images containing a large number of spectra and detail information, spectral and spatial quality are great important for experts to identify the different targets, therefore, we use the correlation coefficient (CC) and degree of the spectral distortion (DSD) to make a quantitative evaluation criterion (ER) of spectral quality besides using the PSNR to evaluate the performance of the denoising results quantitatively.

The correlation coefficient shows similarity in small size structures between the original and processed images, namely indicates the amount of spectral content preserved in the processed images, larger correlation coefficient between the original and denoised image illustrates more spectral content in the denoised image similar to the spectral information of initial image.

The correlation coefficient is defined as

$$\mathrm{Corr}(S,S')=\frac{\sum_{m,n}(S_{mn}-\bar{S})(S'_{mn}-\bar{S}')}{\sqrt{(\sum_{m,n}(S_{mn}-\bar{S})^2)(\sum_{m,n}(S'_{mn}-\bar{S}')^2)}} \tag{13}$$

where $\bar{S}$ and $\bar{S}'$ stand for the mean gray values of original image S and the denoised imageS'.

The degree of the spectral distortion directly reflects the degree of spectral distortion between the original and denoised images, which is defined as follows

$$\mathrm{DSD}=\frac{1}{MN}\sum_i\sum_j|\overline{V(i,j)}-V(i,j)| \tag{14}$$

where M and N are the number of rows and columns respectively, $\overline{V(i,j)}$ and $V(i,j)$ are the pixel gray value of original image and the denoised image located at (i,j). The larger DSD demonstrates more serious spectral distortion in the denoised image, otherwise the spectral quality is better, and its ideal value is zero.

5.1 Noisy panchromatic remote sensing image retrieval

In this section, the panchromatic remote sensing image added zero-mean Gaussian noise with different noise standard deviation σ (30, 35, 40, 45, 50) is denoised using the four denoising approaches.

Table 1 shows the PSNR results for various denoising methods and noise intensities. The results show that the CSCT-TV outperforms CT more than 2 dB, yields 0.5～1.5 dB over CSCT. Furthermore, the CSCT-TV is not only superior 0.5～2.6 dB to TV, but also it can reduce the staircase effect significantly as shown in Fig. 2.

Table 1 PSNR of denoised panchromatic remote sensing images using different algorithms

σ	PSNR/dB				
	Noisy	CT	CSCT	TV	CSCT-TV
30	18.92	19.90	21.13	20.60	22.03
35	17.68	19.22	20.41	20.36	21.47
40	16.62	18.71	19.79	20.15	20.99
45	15.68	18.19	19.17	19.78	20.45
50	14.83	17.77	18.64	19.54	20.03

Table 2 displays the correlation coefficients and degree of the spectral distortion for the different denoising methods.

From the Table 2, in case of different standard deviations, we can see that the CSCT-TV is superior to the other methods in terms of correlation coefficients and degree of the spectral distortion, the CSCT-TV denoising algorithm has more amount of preserved spectral content and less spectral distortion.

Table 2 Correlation coefficients and degree of the spectral distortion of denoised panchromatic remote sensing images for various algorithms

σ	ER	Noisy	CT	CSCT	TV	CSCT-TV
30	DSD	0.089	0.078	0.067	0.068	0.059
	CC	0.891	0.897	0.926	0.915	0.939
35	DSD	0.102	0.085	0.073	0.071	0.063
	CC	0.858	0.879	0.913	0.909	0.931
40	DSD	0.115	0.089	0.079	0.073	0.067
	CC	0.826	0.863	0.899	0.905	0.922
45	DSD	0.129	0.096	0.085	0.076	0.072
	CC	0.791	0.844	0.884	0.895	0.911
50	DSD	0.142	0.101	0.091	0.079	0.075
	CC	0.756	0.826	0.869	0.889	0.902

Fig. 2 shows the denoising result using the CT, CSCT, TV and CSCT-TV denoising algorithms with noise standard deviation $\sigma=30$.

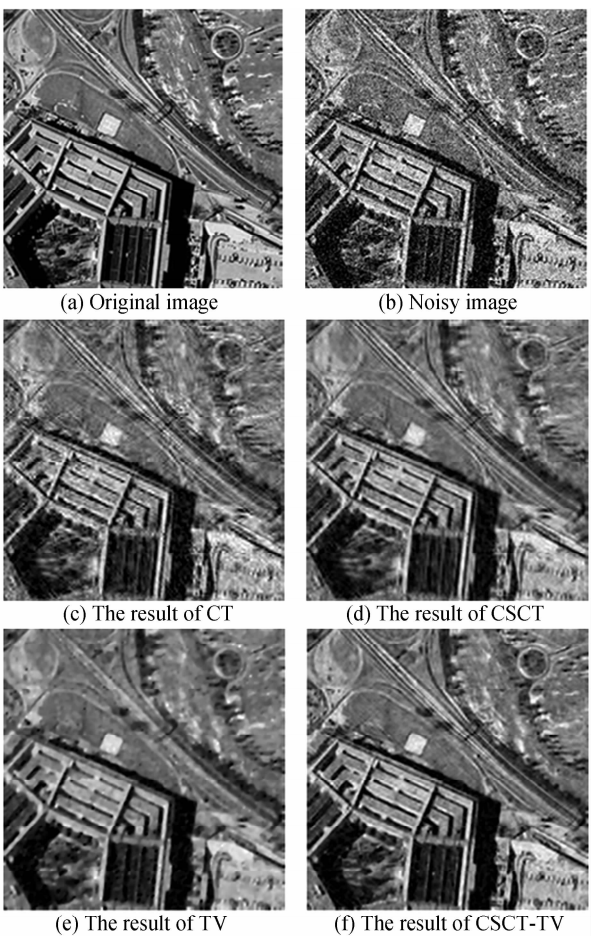

Fig. 2 Denoising results of panchromatic remote sensing image

Comparing the images in Fig. 2(c)～(f), the contours of the building and roads are the most clear in (f). While (c) and (d) blur the building, roads and background for the Gibbs phenomenon, (d) are more distinct than that of (c) for the application of cycle spinning, and (e) appears as many blurs for the staircase effect.

From the Fig. 2 we can see the CSCT-TV obtains better visual effect, and can offer a better recovery of edge information relative to other methods. The CSCT-TV is not capable of reducing Gibbs phenomenon produced by CSCT/CT denoising method, but also weaken the staircase effect caused by TV denoising method.

5.2 Noisy color multi-spectral remote sensing image retrieval

In the second experiment, we implement various denoising approaches for multi-spectral remote sensing image added zero-mean Gaussian noise with different noise standard deviation σ (30, 40, 50).

Table 3 shows the PSNR values after using different algorithms to the original image with zero mean Gaussian white noise and different noise standard deviation.

Table 3 The PSNR values of denoised color remote sensing images implementing different denoising algorithms

σ		PSNR/dB				
		Noisy	CT	CSCT	TV	CSCT-TV
30	R	19.23	22.44	23.02	23.16	24.31
	G	19.01	22.86	22.97	23.11	24.39
	B	18.85	22.22	22.85	23.05	24.48
40	R	16.98	21.19	21.51	22.34	23.32
	G	16.77	21.47	21.51	22.29	23.07
	B	16.63	21.55	21.68	22.32	23.13
50	R	15.29	20.15	20.31	21.50	22.14
	G	15.11	20.29	20.56	21.46	22.00
	B	14.91	20.22	20.49	21.48	21.99

From Table 3, it can be found that the CSCT-TV provides significantly better anti-noise performance than other methods. For the same standard deviation of the Gaussian white noise, the CSCT-TV has a higher R, G, B component PSNR values than other methods.

Table 4 shows the correlation coefficients and degree of the spectral distortion of R, G, B components for the different denoising methods and different noise standard deviation.

As can be seen from the Table 4, the correlation coefficients and degree of the spectral distortion of R, G, B components using CSCT-TV denoising method are all superior to other methods, and the CSCT-TV denoising method can preserve more spectral information and less spectral distortion than others.

Table 4 Correlation coefficients and degree of the spectral distortion of denoised color remote sensing images using different algorithms

σ		ER	Noisy	CT	CSCT	TV	CSCT
30	R	DSD	0.087	0.064	0.054	0.048	0.046
		CC	0.937	0.961	0.971	0.973	0.978
	G	DSD	0.090	0.063	0.053	0.048	0.046
		CC	0.924	0.951	0.964	0.968	0.973
	B	DSD	0.092	0.064	0.054	0.049	0.046
		CC	0.907	0.938	0.955	0.960	0.966
40	R	DSD	0.113	0.073	0.062	0.055	0.053
		CC	0.897	0.947	0.962	0.968	0.971
	G	DSD	0.117	0.074	0.062	0.055	0.054
		CC	0.876	0.935	0.953	0.961	0.964
	B	DSD	0.119	0.074	0.062	0.055	0.053
		CC	0.853	0.918	0.941	0.952	0.956
50	R	DSD	0.136	0.082	0.072	0.062	0.061
		CC	0.852	0.934	0.952	0.960	0.962
	G	DSD	0.141	0.082	0.071	0.062	0.061
		CC	0.825	0.920	0.941	0.952	0.955
	B	DSD	0.145	0.081	0.069	0.062	0.061
		CC	0.793	0.901	0.927	0.942	0.944

Fig. 3 displays the restored multi-spectral remote sensing images after applying CT, CSCT, TV and CSCT-TV with noise standard deviation $\sigma=40$.

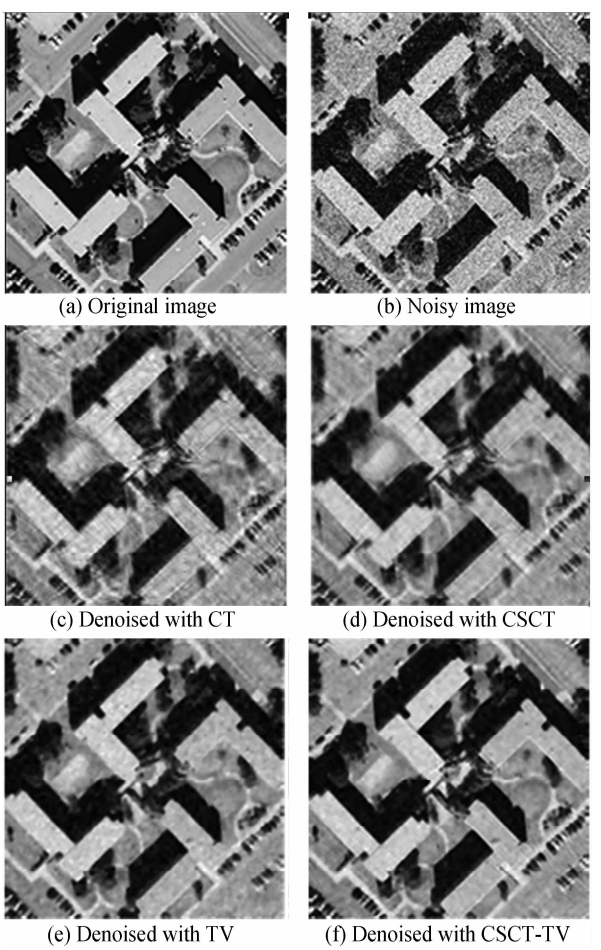

Fig. 3 The restored multi-spectral images after denoising by means of different algorithms

In Fig. 3, as can be seen from the (c) and (d), the cars, trees, roads, building, etc. are blurred, especially the cars are more indistinguishable, (d) are more distinct than that of (c) to a large extent by using cycle spinning, and Gibbs phenomenon is also reduced in (d). From (e), we can see staircase or fragmentation effect and cars, trees and roads are unnatural and not distinct. Comparing the images in Figs. 2(c)～(f), the major components of the (f) is much clearer than that in (c), (d) and (e), and some homogeneous areas (trees, roads, building) become non-homogeneous and not natural.

Based on the results shown in Fig. 2 and Fig. 3, we can see that the proposed method offers better results in restoring the weak edges in the textures, and it is also capable of reducing the Gibbs-like phenomena and staircase effect.

6 Conclusions

For the characteristics of remote sensing image, we proposed an efficient method for remote sensing image denoising. We utilized the cycle spinning algorithm in developing a translation invariant contourlet-based denoising to retrieve more levels of detail and texture contained the remote sensing image, and TV denoising method can preserves large number of edges. Our experiment results clearly demonstrated the capability of the proposed scheme in remote sensing image denoising, and the approach outperforms the CT, CSCT and TV denoising methods both PSNR values, visual and spectral quality.

References

[1] PENNEC E, MALLAT S. Sparse geometric image representation with bandelets[J]. *IEEE Trans on Image Processing*, 2005, **14**(4): 423-438.

[2] DO M N, VETTERLI M. The contourlet transform: an efficient directional multiresolution image representation[J]. *IEEE Trans on Image Processing*, 2005, **14**(12): 2091-2106.

[3] DO M N, VETTERLI M. Contourlet beyond wavelets[M]. WELLAND G V, ed. New York: Academic Press, 2003.

[4] STARCK J, CANDèS E J, DONOHO D L. The curvelet transform for image denoising[J]. *IEEE Trans on Image Processing*, 2002, **11**(6): 670-684.

[5] JIN Wei, WEI Biao, PAN Ying-jun, *et al*. A novel method of neutron radiography image denoising using contourlet transform[J], *Acta Photonica Sinica*, 2006, **35**(5): 760-765.

[6] MIAO Qi-guang, WANG Bao-shu. A novel image fusion method using contourlet transform [C]. *International Conference on Communication, Circuits and System Processing*, 2006, **1**: 548-552.

[7] FENG Peng, PAN Ying-jun, WEI Biao, *et al*. Enhancing retinal image by the Contourlet transform [J]. *Pattern*

Recognition Letters, 2007, **28**(4): 516-522.

[8] XIANG Jing-bo, SU Xiu-qin, LU Tao. Image enhancement based on the contourlet transform and mathematical morphology[J]. *Acta Photonica Sinica*, 2009, **38**(1): 224-227.

[9] WU Yi-quan, XIE Jing, PANG Lei. Multipurpose watermarking algorithm based on krawtchouk moment and contourlet transform[J]. *Acta Photonica Sinica*, 2009, **38**(8): 2160-2164.

[10] COIFMAN R R, DONOHO D L. Translation invariant de-noising, wavelets and statistics[M]. ANTONIADIS A, Oppenheim G, ed. New York: Springer-Verlag, 1994: 125-150.

[11] TAN Li-na, GAO Xie-ping, HE Sheng-ming, *et al*. Study of MRI denoising based on TI multiwavelet thresholding[J]. *Acta Photonica Sinica*, 2007, **36**(8):1552-1556.

[12] ESLAMI R, RADHA H. The contourlet transform for image denoising using cyclic spinning[C]. *Proc of Asilomar Conference on Signals, Systems and Computers, IEEE*, 2003, **2**: 1982-1986.

[13] RUDIN L, OSHER S, FATEMI E. Nonlinear total variation based noise removal algorithms[J]. *Physica D*, 1992, **60**(1-4): 259-268.

[14] GHITA O, ILEA E, WHELAN F. Image feature enhancement based on the time-controlled total variation flow formulation[J]. *Pattern Recognition Letters*, 2009, **30**(3): 314-320.

[15] YIN W, GOLDFARB D, OSHER S. A comparison of three total variation based texture extraction models[J]. *Journal of Visual Communication and Image Representation*, 2007, **18**(3): 240-252.

[16] LIANG D, LI Y, SHEN M. An algorithm for multi-focus image fusion using wavelet based contourlet transform[J]. *Acta Electronica Sinica*, 2007, **35**(2): 320-322.

[17] CAI Xi, ZHAO Wei. Discussion upon effects of contourlet lowpass filter on contourlet-based image fusion algorithms [J]. *Acta Electronica Sinica*, 2009, **35**(3): 258-265.

基于 Cycle Spinning Contourlet 变换和总变分最小化的遥感图像去噪算法

赵杰，杨建雷

（河北大学 电子信息工程学院，河北 保定 071002）

摘　要：针对大部分已有的遥感图像去噪算法在去噪的同时不能有效的保留细节和增强边缘，提出了一种基于 Cycle Spinning Contourlet 变换和总变分最小化的图像去噪新算法. 该算法依据了 Cycle Spinning Contourlet 变换能够很好的保留原始图像的细节和纹理信息，而总变分最小化方法具有在去噪的同时增强图像边缘的特性，因此使用所提出的融合规则对两种算法去噪后的图像进行融合能够取得更好的增强效果. 通过对比，实验结果表明该算法不仅能在很大程度上削弱分别由平移不变 Contourlet 变换和总变分最小化的图像去噪方法产生的伪吉布斯现象和阶梯效应，而且视觉效果和 PSNR 值均优于其它方法，同时该算法能够保留更多的光谱信息，因此该算法是一种有效的遥感图像去噪算法.

关键词：遥感图像；Contourlet 变换；Cycle Spinning；总变分最小化；图像去噪；融合

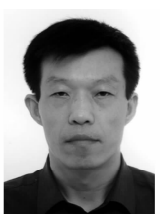

ZHAO Jie was born in 1969. He got his Ph. D. degree from Hebei University of Technology, and now he is a professor and is also the dean of Information Science and Engineering Department of Hebei University. His research interests focus on computer software, image engineering, signal detection and processing.